Universality of strain-induced anisotropic friction domains on 2D materials

Ji Hye Lee[1], Sangik Lee[1], Ji Hoon Jeon[1], Da Yea Oh[1], Minjung Shin[1], Mi Jung Lee[1], Sachin Shinde[2], Jong-Hyun Ahn[2], Chang Jae Roh[3], Jong Seok Lee[3] and Bae Ho Park[1]

Abstract

Van der Waals two-dimensional (2D) materials have shown various physical characteristics depending on their growth methods and conditions. Among those characteristics, the surface structural properties are crucial for the application of 2D materials, as the surface structures readily affect their atomic arrangements and/or interaction with substrates due to their atomic-scale thicknesses. Here, we report on the anisotropic friction domains of MoS_2 grown not only by chemical vapor deposition (CVD) under various sulfur pressure conditions but also by a mechanical exfoliation process. The 180° periodicity of each domain and the 60° shift between adjacent domains indicate the presence of linearly aligned structures along the armchair direction of MoS_2, which is determined by the optical second-harmonic generation method. The anisotropic friction domains of CVD-grown MoS_2 flakes may be attributed to linearly aligned ripples caused by an inhomogeneous strain field distribution, which is due, in turn, to randomly formed nucleation sites on the substrate. The universality of the anisotropic frictional behaviors of 2D materials, including graphene, hBN, and WS_2 with honeycomb lattice stacking, which differ from $ReSe_2$ with a distorted triclinic *1T′* structure, supports our assumption based on the linearly aligned ripples along the crystallographic axes, which result from an inhomogeneous strain field.

Introduction

Two-dimensional (2D) materials are not stable in free-standing forms[1]. However, stable flakes of 2D materials can be obtained through interaction with the substrates. Such interaction gives rise to an inhomogeneous strain in the flakes. As a result, 2D materials exhibit surface corrugations, such as ripples, wrinkles, and bubbles[2–7]. Although such surface corrugations are crucial for the electrical and mechanical properties of 2D materials, the characteristics of the ripples have rarely been revealed, mainly due to their small size and aspect ratio[8]. Friction force microscopy (FFM) is a useful tool to study the characteristics of ripples[9] and periodic deformation[10–12] through the measurement of the local friction on graphene and graphite. Anisotropic friction domains on exfoliated monolayer graphene[13–15], hexagonal boron nitride (hBN)[15], and molybdenum disulfide (MoS_2)[16] have been observed using FFM measurements. However, the origin of the anisotropic friction domains in 2D materials has been debated. In our previous report, we proposed ripple structures aligned along zigzag directions on the graphene lattice, resulting in anisotropic friction domains[13,14]. On the other hand, Gallagher et al. argued that periodic chemical adsorbates on graphene and hBN surfaces might cause anisotropic friction domains[15].

Until now, all the friction domains have been reported in mechanically exfoliated 2D materials. There have been no reports of anisotropic friction domains on 2D materials grown by the chemical vapor deposition (CVD) method. Understanding the physical properties of the nanoscale friction characteristics of 2D materials grown using different methods is crucial for their possible

Correspondence: Bae Ho Park (baehpark@konkuk.ac.kr)
[1]Department of Physics, Division of Quantum Phases and Devices, Konkuk University, Seoul 05029, Korea
[2]Schools of Electrical and Electronic Engineering, Yonsei University, Seoul 03722, Korea
Full list of author information is available at the end of the article

applications as both electronic devices and nanomechanical systems because of their atomic-scale thicknesses.

In this study, we have observed anisotropic friction domains on CVD-grown MoS_2 flakes and mechanically exfoliated 2D materials, such as MoS_2, graphene, hBN, and WS_2 flakes, using FFM measurements. We have proposed that the frictional anisotropic domains on the CVD-grown MoS_2 flakes can be attributed to linearly aligned ripples caused by an inhomogeneous strainfield distribution, which could come from randomly formed nucleation sites on the substrates. It is of particular importance that linearly aligned structures in 2D materials can determine both the major direction of their friction anisotropy and a crystallographic axis of the honeycomb lattice. An extensive FFM study carried out on 2D materials has led us to discover the universality of the frictional anisotropic domains on 2D materials, especially those with honeycomb stacking structures, regardless of the sample growth method used.

Materials and methods
CVD growth of MoS_2

Monolayer MoS_2 crystals were grown by atmospheric-pressure CVD in a two-zone furnace with a 2-inch horizontal quartz tube. Prior to the CVD growth, a Si substrate with 300-nm-thick SiO_2 was cleaned with a water/acetone/IPA sequence and then blow-dried using N_2 gas. In total, 10 mg of molybdenum oxide (MoO_3) powder (≥ 99.5%, Sigma-Aldrich) was loaded in an alumina boat located at the center of the high-temperature furnace zone. Sulfur (≥ 99.5%, Sigma-Aldrich) powder was placed in the upstream region 20 cm away from the center of the MoO_3 zone. The morphology of the MoS_2 crystal changed from a perfect triangle (A) to a multi-arm shape (C) by decreasing the amount of sulfur precursor. The Si wafer was placed face-down above the alumina boat. The temperatures for the MoO_3 and sulfur zones were kept at 750 °C and 200 °C, respectively. A 50/7.5 SCCM Ar/H_2 gas mixture was introduced as a carrier gas to create a reducing atmosphere and promote the reaction. The sulfur zone was preheated and moved when the MoO_3 zone reached 250 °C. The furnace was heated at a ramp rate of 35 °C/min and held at the growth temperature for 15 min. After the growth, the furnace was cooled naturally to room temperature.

Atomic force microscopy (AFM) measurement

FFM and AFM topography images were simultaneously obtained by using the Park Systems XE-100 AFM system in contact mode and in an ambient atmosphere. Both images for each area were obtained to check the effect of the normal force change on the measured friction force. The cantilever loading force of 0.3 nN was fixed during all the measurements. Silicon AFM tips (Nanosensors PPP-

LFMR), with a spring constant of 0.2 N/m and a tip radius of ~10 nm, were used for the imaging. All FFM images were obtained using the longitudinal scan direction (transverse force microscopy, TFM). A sharp silicon probe (MikroMasch Hi'Res-C15/Cr-Au) with a nominal tip radius of ~1 nm and a typical resonant frequency of 325 kHz was used for tapping-mode topography imaging.

Second harmonic generation (SHG) measurement

SHG experiments were carried out with a Ti-sapphire femtosecond laser (Cohernet Vitara-T) with a wavelength of 800 nm, a pulse width of 30 fs, and a repetition rate of 80 MHz. The average power of the pulse was 15 mW, and the probing beam was irradiated on the sample surface with a beam size of 1.29 μm by using a 50× objective lens (0.75 N.A.). The fundamental and SH waves were isolated by using long, short, and band-pass filters. The polarization of each wave was controlled by a half-wave plate and a polarizer. The SH wave intensity was detected by using a photomultiplier tube.

Results and discussion

Three different types of MoS_2 samples, A, B, and C, were grown by the CVD method. From A to C, the sulfur vapor pressure decreased, as we described in the experimental procedures. Sangwan et al. already reported different shapes of CVD-grown MoS_2 flakes depending on the sulfur vapor pressure in a CVD growth process[17]. Figure 1 shows atomic force microscope (AFM) topography and transverse force microscopy (TFM) images of certain flakes on samples A, B, and C. In this study, TFM images were obtained by using the longitudinal scan mode of FFM, where the scanning direction of a probe tip is parallel to the cantilever axis, because it produces much clearer domain contrasts than the conventional lateral scan mode of FFM (lateral force microscopy, LFM) and thus can display the crystallographic orientation in situations where LFM cannot[13,18−20]. The details of TFM have been described in our previous report[12,13] and in the Supporting Information (SI, section A, Figure S1).

Interestingly, domain structures are randomly observed in the TFM images of the sample A (SI, section B, Figure S2). In this sample A, flake M1 (Fig. 1a) does not show a domain structure, whereas flake *a* shows TFM domains (SI, section B, Figure S2(b)). Flakes M2 and M3 (Fig. 1b, c) of samples B and C, respectively, clearly show TFM domains. In the single-crystalline flake M2 without grain boundaries, three distinct TFM domains are observed. The polycrystalline flake M3 with six grains also shows three TFM domains within each single grain. Flakes M1 and M2 do not present any topographical features in the AFM topography (Fig. 1) and optical microscopy images (SI, section C, Figure S4). Each grain of flake M3 does not show topographical structures, either. Therefore, we can
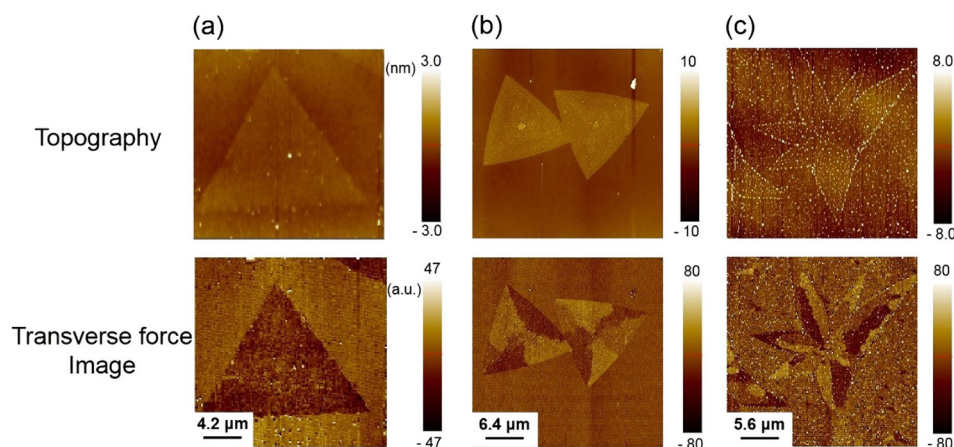
Fig. 1 AFM topography and TFM images of CVD-grown MoS$_2$ flakes. **a** M1, **b** M2, and **c** M3, respectively. Three contrasts of friction domains appear only in flakes M2 and M3

verify that the normal force from the topological structures negligibly affects the friction force measured using longitudinal scan mode in each single grain of our MoS$_2$ samples.

We obtained sample-rotation angle-dependent TFM images of flake M2 by gradually rotating the sample clockwise from 0° to 257° relative to the longitudinal scan direction (black-dashed arrow in Fig. 2a). The brighter contrast in the TFM image indicates a higher transverse force signal. To focus on the friction anisotropy, we normalized the friction force measured from a 2D material by keeping the friction force simultaneously measured from an isotropic SiO$_2$ as 1. Our technique is beneficial to characterizing anisotropic deformations of low-dimensional materials when an isotropic reference material is simultaneously investigated in the TFM measurement. For more information about the samples in this study, we calibrated the torsional response obtained using lateral scan mode (lateral force microscopy, LFM) by the wedge method[21,22] in each sample from the CVD-grown one to the exfoliated one (SI, section F, Figure S9). Polar plots reveal that the TFM signal of each domain has a period of 180° and a shift of 60° with respect to the adjacent domain. Therefore, we can assume that there are linearly aligned structures on the surface of MoS$_2$, whose direction can be determined by the sample-rotation angle-dependent TFM signal (SI, section A). The sinusoidal TFM signal of each domain with a shift of 60° with respect to the adjacent domain can explain our observation that the contrast difference between adjacent domains is not constant but dependent on the sample-rotation angle. As the sample-rotation angle changes, the contrast difference can become weaker and its sign can even be inverted. These behaviors are very similar to what we previously observed on exfoliated monolayer graphene[13,15]. We also

observed three anisotropic domains in sample-rotation angle-dependent TFM images of mechanically exfoliated few-layer MoS$_2$ (Fig. 2b) and few-layer WS$_2$ flakes (SI, section D, Figure S6).

Figure 3 shows the results of the second-harmonic generation (SHG) measurement of flakes M1 and M2. The uniform mapping images of flakes M1 and M2 support that they are single-grain flakes. Fig. 3b, d display the SHG intensity obtained as a function of the sample azimuth with polarizations of the fundamental, and SH waves set to be parallel to each other. A six-fold pattern of the angular dependence is commonly observed, which reflects the hexagonal lattice symmetry (D$_{3h}$) of the MoS$_2$ flakes[23]. Furthermore, there were no considerable peak shifts in the Raman spectroscopic data of flakes M1 and M2 (SI, section C, Figure S5). These results indicate that the lattice configurations of the two flakes do not have any deformation. The crystal orientation of flake M2 is determined by the dependence of the SHG intensity on the azimuthal angle (θ) with respect to the armchair direction of the MoS$_2$ lattice, which is given as $(\sin 3\theta)^2$[24]. The experimental results can be fit well, as indicated by the solid line in Fig. 3d, and the armchair direction of the MoS$_2$ lattice is determined to be that with the minimum SHG intensity. By comparing these results with the TFM images in Fig. 2a, it is found that the ripples of MoS$_2$ flake M2 are aligned along the armchair direction of the lattice (Fig. 3e).

In the recent literature, frictional behaviors have been investigated in several 2D materials, such as mechanically exfoliated graphene[13–15], hBN[15], and MoS$_2$[16] flakes. Notably, an angle shift of ~60° between each friction domain was also reported in these references. We also observed TFM domains with only three distinctive contrasts in the exfoliated MoS$_2$ (Fig. 2 and S7), WS$_2$
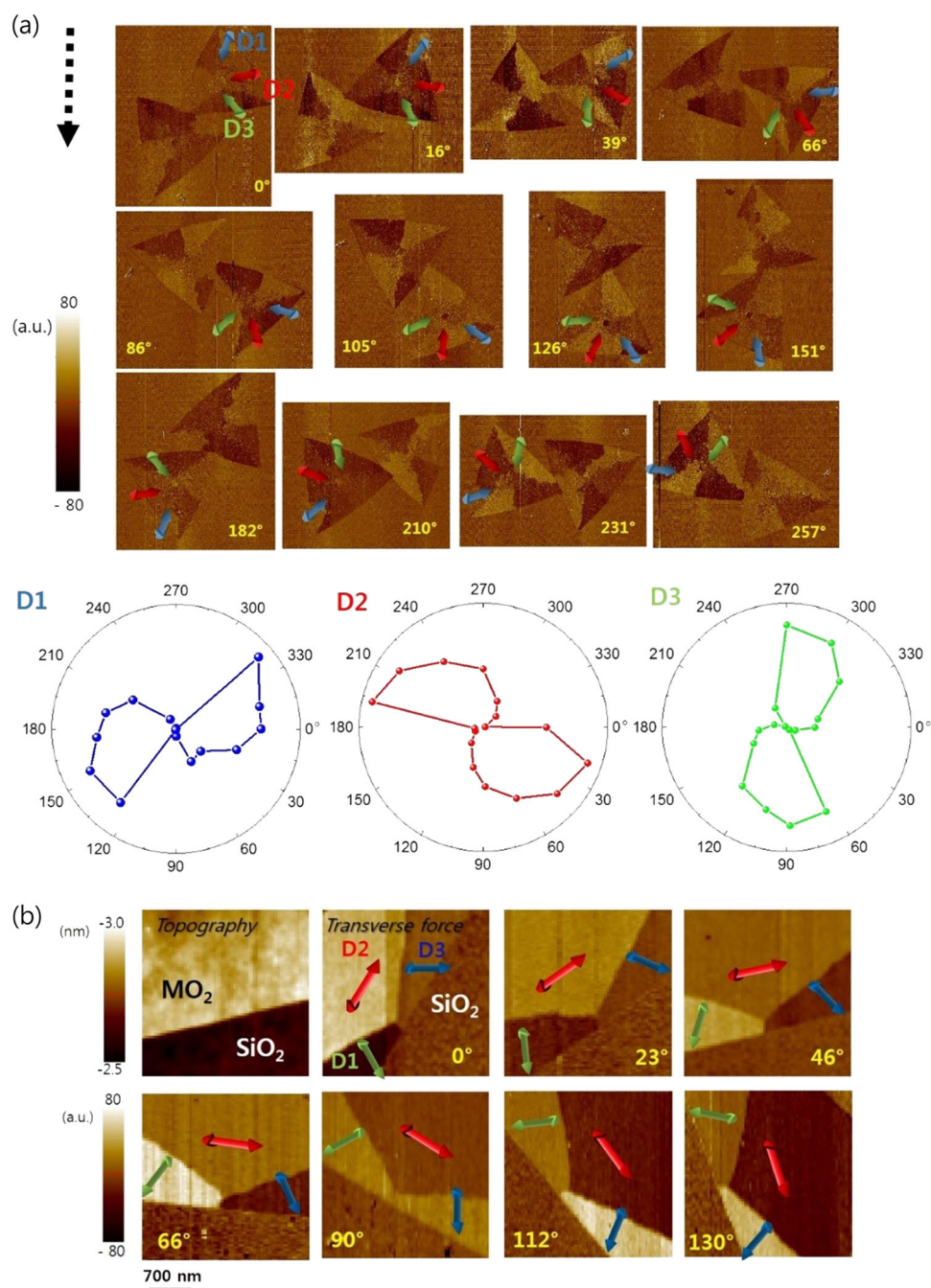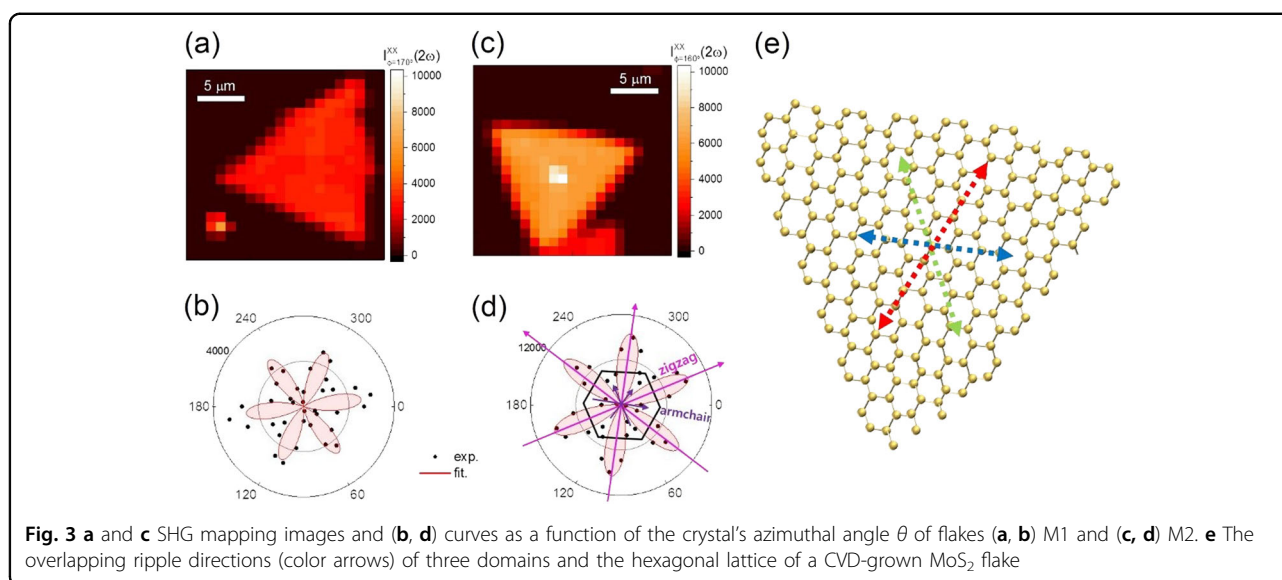
Fig. 2 a Sample-rotation angle dependent TFM images and polar plots of TFM signals at three domains of CVD-grown MoS$_2$ flake M2. The colored arrows represent the ripple directions of three domains. The black-dashed arrow denotes the scan direction of the cantilever. **b** Sample-rotation angle-dependent TFM images of a mechanically exfoliated MoS$_2$ flake on a SiO$_2$ substrate

(Figure S6), and thick-hBN flakes (SI, section E, Figure S8). Hence, one could expect that the 60° shift of each TFM domain is related to the corresponding lattice configuration because graphene, hBN, WS$_2$, and MoS$_2$ have honeycomb lattice structures. To confirm this relation, we performed the same measurement for another 2D material, few-layer of mechanically exfoliated ReSe$_2$, which has a distinct distorted triclinic *1 T'* structure[25] (SI, section G, Figure S10). The ReSe$_2$ sample did not show any distinguishable TFM domains having different contrasts (Figure S10(a)), whereas the anisotropic TFM signal on each flake had a 180° periodicity, verified by incrementally rotating the sample clockwise (Figure S10(b)). Therefore, we can conclude that the TFM signal might be induced by

Fig. 3 a and **c** SHG mapping images and (**b, d**) curves as a function of the crystal's azimuthal angle θ of flakes (**a, b**) M1 and (**c, d**) M2. **e** The overlapping ripple directions (color arrows) of three domains and the hexagonal lattice of a CVD-grown MoS₂ flake

a linearly aligned structure along a certain crystallographic direction of the 2D material.

As mentioned above, in terms of the origin of the anisotropic frictional signal on 2D materials, there are two controversial interpretations of these linearly aligned structures. Gallagher et al. argued that the periodic adsorbates (wavelength of 4–6 nm) on the surface of graphene and hBN could result in anisotropic frictional behaviors when exposed to the ambient air during the growth process and/or several measurements[15]. However, in our study, we may be able to exclude periodic adsorbates. If the assumption of periodic adsorbates could be applied to our case, all the flakes in one sample should show similar TFM domain characteristics: the other flakes of a sample in which one flake showed friction domains should also show friction domains. However, we could observe TFM domains randomly distributed in sample A: some flakes showed TFM domains, whereas others did not. Moreover, our sample A has not changed for a long time since its exposure to air: there are still no TFM domains in flakes M1 (Fig. 1a) and *b* (SI, section B, Figure S2) after a few months since its initial growth (SI, section B, Figure S3). If TFM domains would result from adsorbates that could be distributed evenly after a long exposure to air, friction domains should appear even in a flake that did not show TFM domains initially due to the randomly distributed adsorbates. We can expect that the CVD-grown MoS₂ flakes have different strain distributions due to either different states of substrates or different nucleation patterns during the CVD growth. Therefore, we speculate that the anisotropic friction domains in 2D materials result from strain-induced ripple structures with very small aspect ratios, which have been rarely detected in transmission electron microscopy

(TEM) measurements[26,27]. Even in tapping-mode AFM topography images obtained using a sharp probe tip (tip radius ~1 nm), we could not observe any periodic patterns (SI, section H, Figure S11). This result indicates that the ripple structures are far beyond our AFM resolution. It is expected that the friction anisotropy originates from very smooth ripples with very low aspect ratios (< 1/10) between height (~Å) and width (~nm)[28].

The local strain field distribution and resultant ripple structures can be affected by the interaction with a substrate. To investigate this, thermal annealing was carried out for a flake in sample B at different temperatures in a high vacuum of 1.2 × 10⁻⁶ Torr, and then the flake was exposed to air before the TFM measurement. Figure 4 shows that the TFM domain becomes weaker after thermal annealing at 300 °C, and it completely disappears after annealing at 350 °C. If adsorbates would induce TFM domains, they could be detached from the flake during vacuum annealing but reversibly attached to it after exposure to air, leading to the redistribution of the TFM domains. Alternatively, thermal annealing might release an inhomogeneous strain field on the MoS₂ flake, which is probably induced by different states of the substrate and/or conditions of the CVD deposition process. In addition, the experiment of transferring flakes to another substrate (SI, Section I, Figure S12) could support our scenario, in which the modulation of the local strain field resulted in changes in the TFM signals of the flakes.

We should note that three distinctive friction domains appear universally in 2D materials with a hexagonal honeycomb structure. Our observations support that this could originate from linearly aligned ripple structures, while the Gallagher group's observations indicated that this might be caused by periodic chemical adsorbates. In
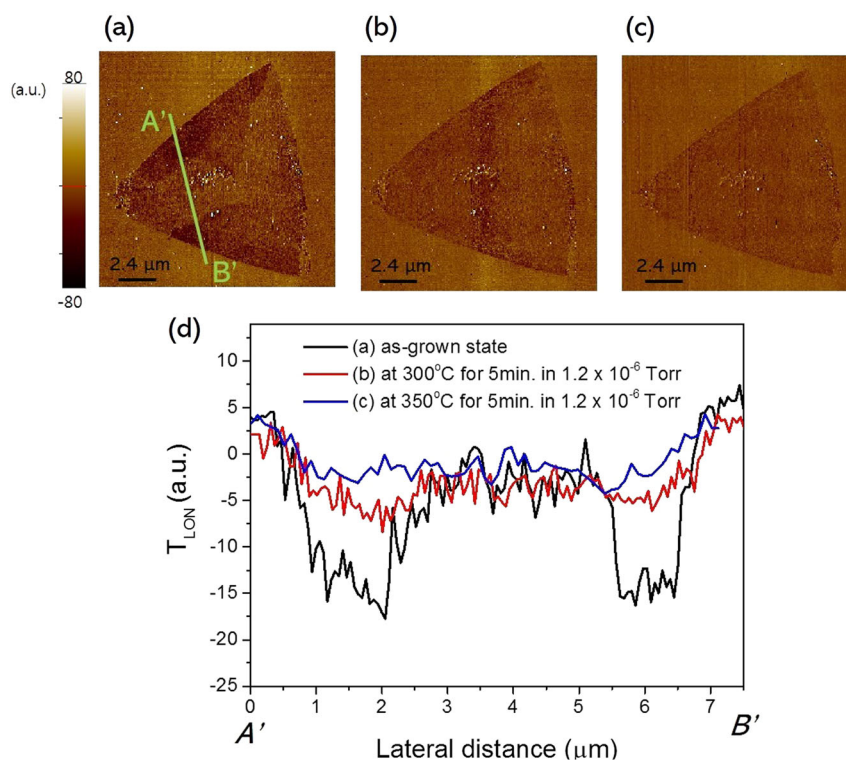
Fig. 4 TFM images of a CVD-grown MoS_2 flake in sample B (**a**) in the as-grown state, (**b**) after annealing at 300 °C for 5 min, and (**c**) after again annealing at 350 °C for 5 min. **d** Line profiles of TFM signals between points *A'* and *B'* marked in **a**

both cases, the corresponding structural deformation is lined with a certain crystallographic major direction of a 2D material, which could be used to determine the crystallographic orientation of the 2D material.

Conclusion

In summary, we have investigated the universal characteristics of nanoscale friction domains in 2D materials, such as graphene, hBN, WS_2, and MoS_2 with a hexagonal honeycomb structure. It has been found that friction domains can be observed not only in mechanically exfoliated flakes of 2D materials but also in CVD-grown MoS_2. In a CVD-grown MoS_2 flake, the TFM signal shows a periodicity of 180°, which originates from a linearly aligned structure. Such a structure has been determined using SHG measurements to be along the armchair direction of MoS_2. We can suggest the universality of the anisotropic frictional characteristics on van der Waals 2D materials, which is induced by linearly aligned structures along a crystallographic axis of the honeycomb lattice structure. Understanding and controlling the nanomechanical features of the surfaces of 2D materials is fascinating and crucial: such properties not only have a significant impact on the electrical behavior of low-dimensional materials, but they can also be exploited for several future applications.

Author details
[1]Department of Physics, Division of Quantum Phases and Devices, Konkuk University, Seoul 05029, Korea. [2]Schools of Electrical and Electronic Engineering, Yonsei University, Seoul 03722, Korea. [3]Department of Physics and Photon Science, Gwangju Institute of Science and Technology (GIST), Gwangju 61005, Korea

Conflict of interest
The authors declare that they have no conflict of interest.

Publisher's note
Springer Nature remains neutral with regard to jurisdictional claims in published maps and institutional affiliations.

Supplementary information is available for this paper at https://doi.org/10.1038/s41427-018-0098-2.

References

1. Rabe, J. P. & Buchholz, S. Commensurability and mobility in two-dimensional molecular patterns on graphite. *Science* **253**, 424–427 (1911).
2. Fasolino, A., Los, J. H. & Katsnelson, M. I. Intrinsic ripples in graphene. *Nat. Mater.* **6**, 858–861 (2007).
3. Lui, C. H., Liu, L., Mak, K. F., Flynn, G. W. & Heinz, T. F. Ultraflat graphene. *Nature* **462**, 339 (2009).
4. Khestanova, E., Guinea, F., Fumagalli, L., Geim, A. K. & Grigorieva, I. V. Universal shape and pressure inside bubbles appearing in van der Waals hetero-structures. *Nat. Commun.* **7**, 12587 (2016).
5. Zang, J. et al. Multifunctionality and control of the crumpling and unfolding of large-area graphene. *Nat. Mater.* **12**, 321–325 (2013).
6. Chae, S. J. et al. Synthesis of large-area graphene layers on poly-nickel substrate by chemical vapor deposition: wrinkle formation. *Adv. Mater.* **21**, 2328–2333 (2009).
7. Levy, N. et al. Strain-induced pseudo-magnetic fields greater than 300 Tesla in graphene nanobubbles. *Science* **329**, 544–547 (2010).
8. Tapaszto, L. et al. Breakdown of continuum mechanics for nanometer-wavelength rippling of graphene. *Nat. Phys.* **8**, 739–742 (2012).
9. Lee, C. et al. Frictional characteristics of atomically thin sheets. *Science* **328**, 76–80 (2010).
10. Rastei, M. V., Heinrich, B. & Gallani, J. L. Puckering stick-slip friction induced by a sliding nanoscale contact. *Phys. Rev. Lett.* **111**, 084301 (2013).
11. Rastei, M. V., Guzmán, P. & Gallani, J. L. Sliding speed-induced nanoscale friction mosaicity at the graphite surface. *Phys. Rev. B* **90**, 041409(R) (2014).
12. Dienwiebel, M., Verhoeven, G. S., Pradeep, N. & Frenken, J. W. M. Superlubricity of graphite. *Phys. Rev. Lett.* **92**, 126101 (2004).
13. Choi, J. S. et al. Friction anisotropy-driven domain imaging on exfoliated monolayer graphene. *Science* **333**, 607–610 (2011).
14. Choi, J. S. et al. Facile characterization of ripple domains on exfoliated graphene. *Rev. Sci. Instrum.* **83**, 073905 (2012).
15. Gallagher, P. et al. Switchable friction enabled by nanoscale self-assembly on graphene. *Nat. Commun.* **7**, 10745 (2016).
16. Boland, M. J., Nasseri, M., Patrick Hunley, D., Ansary, A. & Strachan, D. R. Striped nanoscale friction and edge rigidity of MoS_2 layers. *RSC Adv.* **5**, 92165–92173 (2015).
17. Sangwan, V. K. et al. Gate-tunable memristive phenomena mediated by grain boundaries in single-layer MoS_2. *Nat. Nanotech.* **10**, 403–406 (2015).
18. Kalihari, V., Tadmor, E. B., Haugstad, G. & Frisbie, C. D. Grain orientation mapping of polycrystalline organic semiconductor films by transverse shear microscopy. *Adv. Mater.* **20**, 4033–4039 (2008).
19. Campione, M. & Fumagalli, E. Friction anisotropy of the surface of organic crystals and its impact on scanning force microscopy. *Phys. Rev. Lett.* **105**, 166103 (2010).
20. Flesch, H.-G. et al. Microstructure and phase behavior of a quinquethiophene-based self-assembled monolayer as a function of temperature. *J. Phys. Chem. C.* **115**, 22925–22930 (2011).
21. Ogleterr, D., Carpick, R. W. & Salmeron, M. Calibration of frictional forces in atomic force microscopy. *Rev. Sci. Instrum.* **67**, 3298–3306 (1996).
22. Varenberg, M., Etsion, I. & Halperin, G. An improved Wedge calibration method for lateral force in atomic force microscopy. *Rev. Sci. Instrum.* **74**, 3362–3367 (2003).
23. Molina-Sánchez, A. & Wirtz, L. Phonons in single-layer and few-layer MoS_2 and WS_2. *Phys. Rev. B* **84**, 155413 (2011).
24. Kumar, N. et al. Second harmonic microscopy of monolayer MoS_2. *Phys. Rev. B* **87**, 161403(R) (2013).
25. Jariwala, B., Thamizhavel, A. & Bhattacharya, A. ReS_e2: a reassessment of crystal structure and thermal analysis. *J. Phys. D. Appl. Phys.* **50**, 044001 (2017).
26. Brivio, J., Alexander, D. F. L. & Kis, A. Ripples and layers in ultrathin MoS_2 membranes. *Nano. Lett.* **11**, 5148–5153 (2011).
27. Wang, W. L. et al. Direct imaging of atomic-scale ripples in few-layer graphene. *Nano. Lett.* **12**, 2278–2282 (2012).
28. Morozov, S. V. et al. Strong suppression of weak localization in graphene. *Phys. Rev. Lett.* **97**, 016801 (2006).